Volume 24, No 1 | International Journal of Radiation Research, January 2026

Influence of bolus materials on dose deposition in electron beam radiotherapy: A Monte Carlo simulation

D. Kong, L. Hui, B. Yang, J. Huang, Y. Zhao, K. Gu*

Department of Radiation Oncology, Affiliated Hospital of Jiangnan University, WUXI 214122, China

► ***Original article***

Corresponding author:
Ke Gu, Ph.D.,
E-mail: *pilipolome@126.com*

Received: January 2025
Final revised: August 2025
Accepted: August 2025

Int. J. Radiat. Res., January 2026; 24(1): 25-30

DOI: 10.61186/ijrr.24.1.4

Keywords: *Monte Carlo method, elastomeric polymer, radiation dosage, electrons.*

ABSTRACT

Background: This study employed Geant4 to evaluate the comparative effects of various bolus materials on dose deposition during electron beam radiotherapy. ***Materials and Methods:*** A bolus was simulated in Geant4, positioned 100 cm away from the accelerator source, with dimensions of 30 cm × 30 cm and varying thicknesses. The materials tested included water, glycerol, polystyrene, and silica gel. A tissue-equivalent phantom was positioned adjacent to the bolus, and voxels were incorporated to measure dose deposition as 6 and 9 MeV electron beams passed through it. The analysis focused on comparing maximum doses, effective therapeutic depths (ETDs), and dose distributions beyond the ETD. ***Results:*** The depth of maximum dose (d_{max}) showed a linear relationship with increasing bolus thickness, moving closer to the phantom surface with material-specific coefficients. The onset depth of the ETD decreased progressively until it reached the phantom surface. For equivalent bolus thicknesses where the ETD did not initial at the surface, the ETD regions exhibited similar dimensions, with onset depths in the order: silica gel < glycerol < water < polystyrene. When the ETD began at the surface, the size of the ETD regions followed the same order. The relative dose beyond the ETD generally followed the order: silica gel > water > glycerol > polystyrene. ***Conclusion:*** Bolus materials exert a significant influence on dose distribution in electron beam radiotherapy.

INTRODUCTION

Megavolt electron beams and X-rays exhibit a dose build-up effect, resulting in reduced superficial dose. For the treatment of superficial tumors, a bolus, defined as a tissue-equivalent material, is essential for improving dose conformance and uniformity while minimizing radiation exposure to normal tissue [1-3]. Air gaps between the bolus and the skin surface can adversely affect superficial dose delivery. Sharma *et al*. showed that superficial dose decreases with increasing cavity gap size, decreasing electron beam energy, smaller radiation fields, and thicker boluses using polystyrene bolus [4]. Huang *et al.* employed a rigid solid water HE plate as bolus material and observed that when the cavity thickness reached 5 mm in a magnetic resonance-guided accelerator, the epidermal dose dropped to half the predicted value, which differed significantly from results using conventional accelerators [5]. Mahdavi *et al*. demonstrated that air cavities between the bolus and skin in volumetric modulated arc therapy (VMAT) plans led to insufficient dose to superficial target areas [6]. 3D printing technology is increasingly being applied to create boluses. Su *et al*. [7] and Junfeng *et al.* [2] utilized PLA as a material to create 3D-printed boluses for modulating dose distribution in electron beam therapy. Li *et al*. demonstrated the effectiveness of reducing the distance between bolus and skin by applying water-equivalent polymers and CBCT scanning to generate 3D-printed boluses [3]. Song and Li confirmed the benefits of 3D-printed boluses made with FDM thermoplastic polyurethane (TPU 92A), reporting improvements in surface conformity and dose parameters using intensity-modulated radiotherapy (IMRT) plans in the Eclipse radiotherapy planning system (TPS) [8]. Won and Kim demonstrated dosimetric variation caused by different fillers in 3D-printed molds [9]. Wang *et al*. validated the superiority of custom silicone rubber boluses over conventional ones using CT scans and optically stimulated luminescent dosimeter measurements [10]. Numerous materials are available for bolus fabrication. Traditional hand-made boluses include water, wet gauze, paraffin, petroleum jelly, dental mold materials, thermoplastics, superabsorbent polypropylene and rayon cloth, and metals. Commercial products include Superflab and Super-Flex. Materials for 3D-printed boluses include acrylonitrile butadiene styrene (ABS), TPU, polymers, silicone, and hydrogel [11]. According to radiation interaction theory, the composition and type of bolus material substantially influence dose distribution, particularly in shallow tissue. Kyeong-Hyeon *et al*. reported the thickness of silica-gel bolus can be equivalent to 1.06 and 1.07 times of water bolus for 6 and 9 MeV electron beams, respectively [12]. Okoh *et al*. compared a polyvinyl alcohol (PVA) based bolus to standard bolus material, observing minimal differences in percentage depth dose (PDD) and

[DOI: 10.61186/ijrr.24.1.4]

superficial dose in solid water phantoms, regardless of PVA content [13]. While these studies offer useful guidance for bolus selection, experimental data alone are insufficient. Moreover, solid water, commonly used as a water-equivalent phantom material, continues to evolve and dose not perfectly replicate the composition of human tissue [14]. Therefore, measurements based on solid water phantoms may not provide a completely accurate representation of dose changes in the body.

The primary objective of this study is to investigate the effects of four commonly used bolus materials-water, glycerol (the primary component of petroleum jelly), polystyrene, and silica gel-on the dose distribution of electron beams in tissues by employing theoretical modeling, Geant4 Monte Carlo simulation [15-17], and subsequent data analysis. The study will provide radiotherapists and physicists with a reference guide for planning radiotherapy treatments involving the use of bolus.

This study's innovation lies in the development of a model that more accurately represents clinical treatment scenarios. It provides detailed data on the influence of bolus materials on surface dose during electron beam radiotherapy, including dose behavior beyond the effective therapeutic depth (ETD).

MATERIALS AND METHODS

Constructing bolus and tissue phantom

The experimental model used in this study is illustrated in figure 1. The bolus was positioned at the source axis distance (SAD) of 100 cm, with a surface area of 30 cm× 30 cm. The thickness and material of the bolus varied according to the study objectives. A tissue phantom measuring 30 cm× 30 cm× 30 cm was placed beneath the bolus. The skin was in direct contact with the bolus and thus experienced the most significant material effects. To minimize the influence of dose re-build-up between different tissues in the phantom, the entire phantom was modeled using skin tissue (G4_SKIN_ICRP [18]) as the medium. Additionally, to reduce calculation errors caused by cavity effects, the bolus was kept in close contact with the phantom. The centers of the bolus and phantom were aligned with the central axis of the radiation field, and a 10 cm × 10 cm electron beam field was used to irradiate both. Voxels were defined along the central axis to record the deposited dose. To reduce calculation error, all voxel cross-sectional areas were set to 1.0 cm × 1.0 cm, with voxel thicknesses of 0.1 cm within the upper 3 cm of the phantom and 0.5 cm beyond that depth. Bolus thicknesses of 0.3 cm, 0.5 cm, 1.0 cm, 1.5 cm, and 2.0 cm were constructed using water (G4_WATER [18]), glycerol (G4_GLYCEROL [18]), polystyrene (G4_POLYSTYRENE [18]), and silica gel. The silica gel had a density of 1.155 g/cm^3 and was composed of hydrogen (8.11% by mass), carbon (32.43%), oxygen (21.62%), and silicon (37.84%).

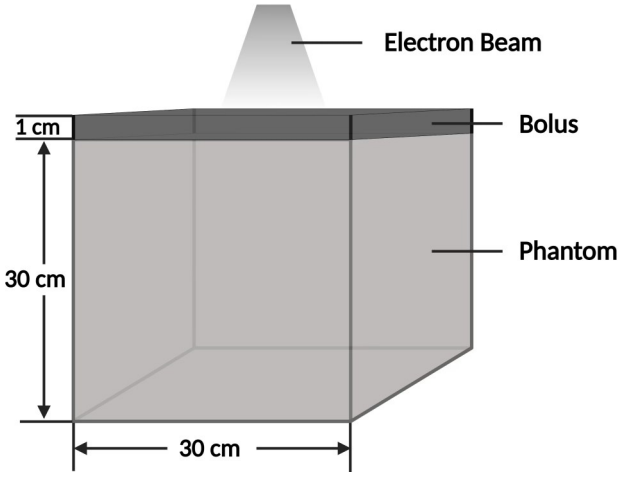

Figure 1. Model of electron beam irradiation.

Geant4 runtime platform and electron beam source

Simulations were conducted on a 64-bit Windows 10 operating system (Microsoft, Redmond, USA) using Microsoft Visual Studio Community 2019 (version 16.10.2) as the C++ compiler. The Geant4 Monte Carlo simulation toolkit (version 10_07_p02) (European Organization for Nuclear Research, Geneva, Switzerland) was used to calculate energy deposition. The study focused on the clinical use of 6 and 9 MeV electron beams, and therefore, the initial particle source used the phase space files (PSFs) of 6 and 9 MeV electron beams with a field of 10 cm×10 cm, produced by Varian Clinac 2100CD medical linear accelerator. These PSFs was obtained from the official website of the International Atomic Energy Agency (IAEA) [19].

Dose deposition in the phantom

The particle transportation and dose deposition were simulated using Geant4 with the LowE_Livermore physics model, with a default cut-off range of 1 mm. The PSFs described above were used as the initial particle sources, with all particles sampled simultaneously. The 6 MeV electron beam used 56,871,296 initial particles [20], and the 9 MeV beam used 56,197,810 [20]. A 160 mm × 160 mm × 1 mm plane located 30 mm above the bolus (970 mm from the virtual source of the accelerator) recorded phase space data and generated new PSFs, which were used to simulate 1.6 ×10^9 particles in the model. To reduce calculation error, geometrical importance sampling was employed with assigned weight values of 1 (world), 10 (nearby environment), 100 (bolus and phantom), and 1000 (voxels). The deposited dose and its associated error were recorded for each voxel.

Data processing and visualization

To determine the PDD in the phantom for various bolus thicknesses, the maximum dose within the

[DOI: 10.61186/ijrr.24.1.4]

phantom was used for normalization. The effective therapeutic dose was defined as 90% of the maximum dose [21], and the corresponding depth was defined as the ETD. For dose comparisons beyond the ETD, accurate determination of the ETD cut-off was necessary. Since the depth often fell between voxels and varied with bolus material, a precise interpolation method was required to determine the dose and its depth beyond the d_{max}. Akima interpolation was used to generate smooth curves through all reference points without assuming a specific functional form [22]. This method minimized the accumulation of errors of those reference points and prevented curve oscillations. Akima interpolation was performed using OriginPro 2018C (64-bit) (OriginLab, Northampton, USA) to interpolate PDDs after d_{max}. For 6 MeV electron beams, the interpolation range was between 17 mm and 38 mm, and the reference range was between 15 mm and 45 mm, with 211 interpolation points. For 9 MeV electron beams, the interpolation range was between 27 mm and 51 mm, and the reference range was between 24 mm and 60 mm, with 241 interpolation points. Linear interpolation was used to determine the ETD cut-off for each bolus thickness. To compare dose distributions beyond the ETD among different bolus materials, all doses were normalized to the dose at the corresponding depth for a water bolus of the same thickness.

RESULTS

Maximum dose in tissues

The d_{max} for both electron beam energies decrease linearly with increasing bolus thickness, but the coefficient varies for different bolus materials until d_{max} reaches the surface of the phantom, as shown in figure 2. If d_{max} is not on the surface, then the order of d_{max} for the same electron beam energy and bolus thickness is silica gel < glycerol < water < polystyrene. Table 1 presents the maximum relative dose in the phantom with bolus of different thicknesses and materials at 6 and 9 MeV electron beams. The table reveals that as the bolus thickness increases and before the maximum dose reaches the phantom surface, polystyrene causes a decrease in the maximum dose, while silica-gel leads to an increase, but the maximum change is only about 2%.

Effective therapeutic depths (ETD)

Figure 3 depicts the ETD of electron beams in the phantom with different bolus materials, where the solid black line and gray dot line indicate the starting and cut-off depth of the ETD, respectively. The effective therapeutic region is between these two lines. From the figure, we can observe that if the ETD does not start from the surface of the phantom, the effective therapeutic region with different bolus materials is almost the same in size, but there are some differences between the starting depths of the effective therapeutic region with different bolus materials. If bolus materials have the same thickness, the effective therapeutic starting depth in a phantom is silica gel bolus < glycerol < water < polystyrene. If the ETD starts from the surface of the phantom, the effective therapeutic region decreases rapidly with increasing bolus thickness, and for the same bolus thickness, the effective treatment region in a phantom is silica gel bolus < glycerol < water < polystyrene.

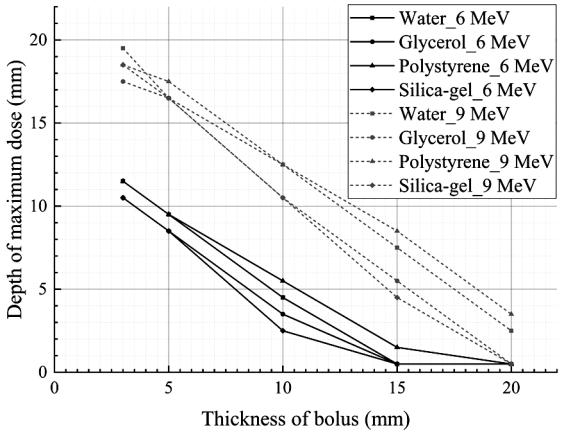

Figure 2. Depth of maximum dose in phantom with different bolus.

Table 1. Maximum relative dose in phantom with different bolus at the irradiation of 6 MeV and 9 MeV electron beams.

Energy	Bolus thickness (mm)	Bolus materials			
		Water	Glycerol	Polystyrene	Silica-gel
6 MeV	3	99.79±0.12	99.81±0.12	99.83±0.12	99.88±0.12
	5	99.64±0.12	99.84±0.12	99.47±0.12	99.89±0.12
	10	99.55±0.12	99.81±0.12	99.27±0.12	101.06±0.12
	15	99.81±0.12	94.86±0.12	98.49±0.12	96.47±0.12
	20	86.71±0.12	57.32±0.09	87.76±0.12	62.50±0.09
9 MeV	3	99.74±0.13	100.06±0.13	99.89±0.13	99.94±0.13
	5	99.80±0.13	99.88±0.13	99.67±0.13	100.02±0.13
	10	99.55±0.13	99.84±0.13	99.51±0.13	100.14±0.13
	15	99.54±0.13	99.96±0.13	99.18±0.13	100.97±0.13
	20	99.61±0.12	99.86±0.13	98.83±0.12	102.07±0.13

Values are expressed as means ± standard deviations. These values have been normalized to the maximum dose in the phantom without bolus.

Tissue dose after the ETD

Figure 4 illustrates the relative dose distributions of electron beams in the phantom with different bolus materials, after the depth of ETD. To minimize errors caused by simulation and interpolation, only the range of depth where all PDDs are > 5% is considered. For the four bolus materials, the ranges for 6 and 9 MeV electron beams are 11 and 16 mm after the ETD, respectively. For 6 MeV electron beams, the relative dose in that range varies significantly with different bolus materials. At the same depth, the relative dose of silica gel is the highest, while that of polystyrene is the lowest, and glycerol has a higher dose than water. The differences increase with the increase of depth in the phantom and of bolus thickness. The differences in the relative dose of 9 MeV electron beams with different bolus

[DOI: 10.61186/ijrr.24.1.4]

materials are similar to those of 6 MeV, but they are smaller. In the range of interest, the relative dose curve with a silica-gel bolus shows a small fluctuation with the increase of depth in the phantom initially and then increases rapidly. On the other hand, the relative dose with a glycerol bolus rises quickly when approaching the boundary of the range, even higher than the dose in the phantom with a water bolus.

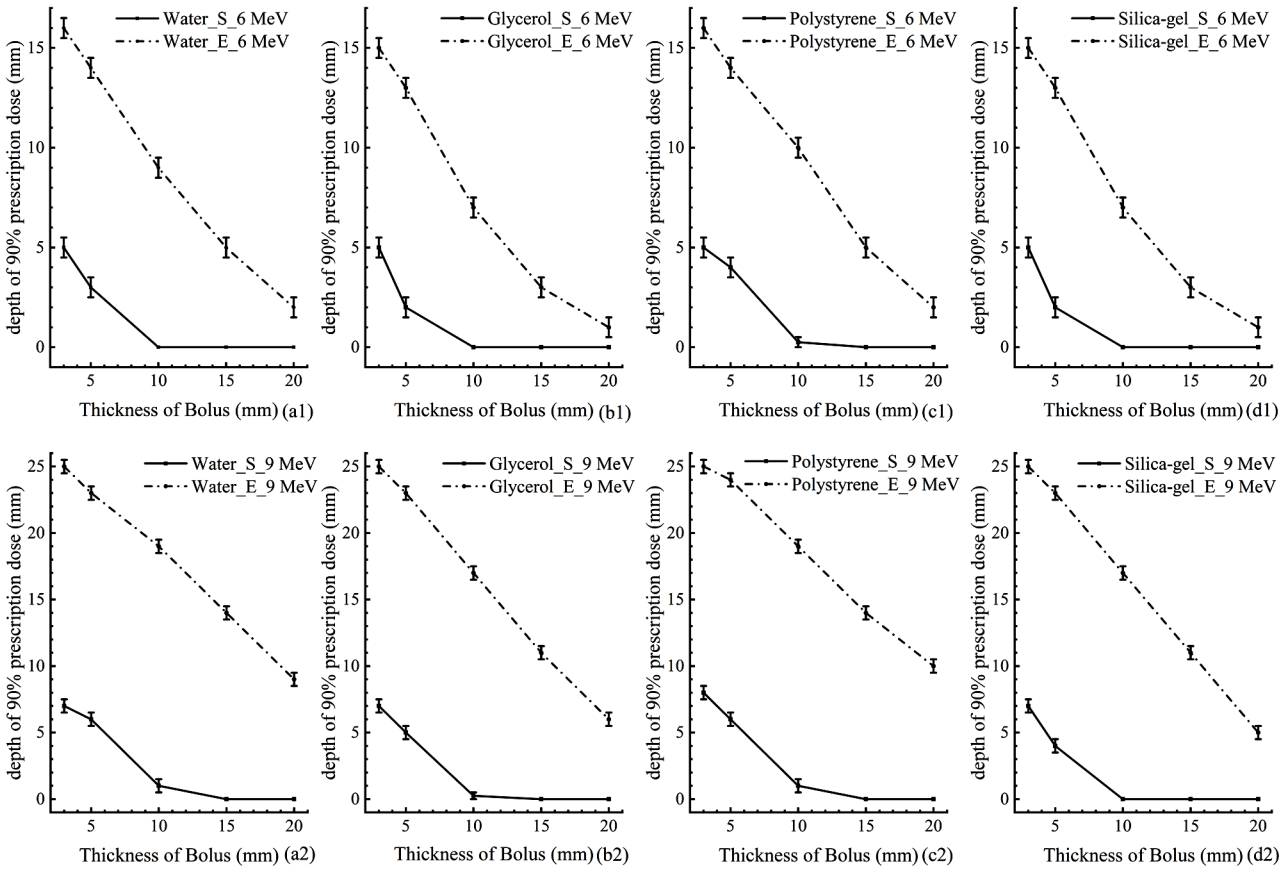

Figure 3. Comparison of the effective therapeutic depths (ETDs) in phantom with different bolus at the irradiation of 6 MeV and 9 MeV electron beams, the maximum dose on the central axis of the field is selected as the prescribed dose, and 90% of the prescribed dose is set as the effective therapeutic dose, the corresponding depth is as the ETD (S represents the starting depth of ETD, and E represents the cut-off depth of ETD).

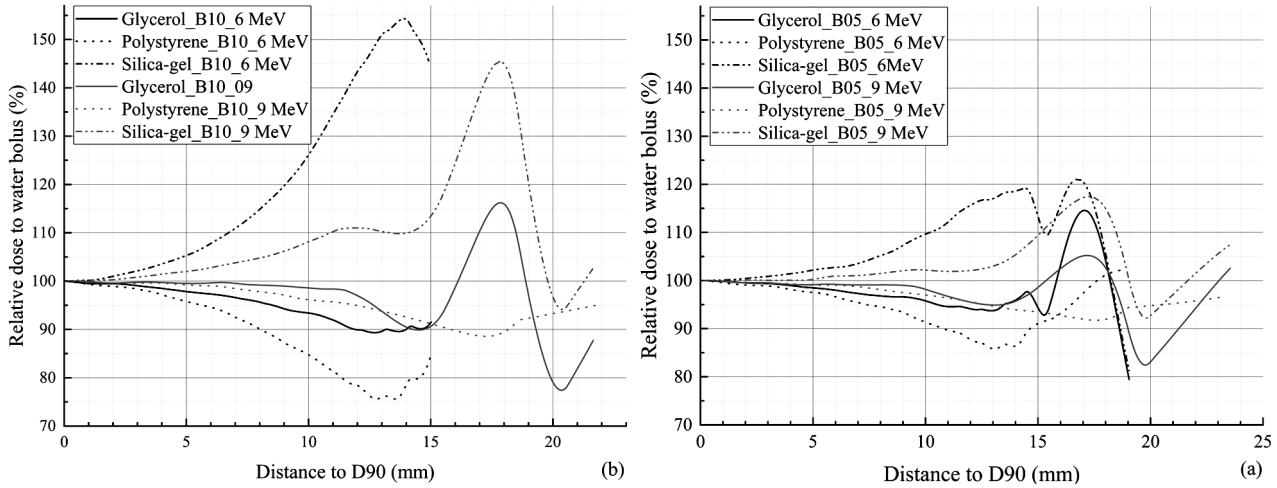

Figure 4. Comparison of relative dose distributions after effective therapeutic depth in phantom with different materials bolus at the irradiation of 6 MeV and 9 MeV electron beams (**(a)** the thickness of bolus is 5 mm; **(b)** the thickness of bolus is 10 mm. The dose in each point is normalized to the corresponding dose in phantom with water bolus).

[DOI: 10.61186/ijrr.24.1.4]

DISCUSSION

This study demonstrated that, irrespective of the bolus material used, the d_{max} in the phantom decreases, consistent with previous reports [12, 13, 23]. The correlation observed between the d_{max} values for silica-gel and water boluses aligns with the findings of Kim *et al*. [12]; however, the ratio in the present study is approximately 1.2, potentially due to differences in silica-gel composition, electron beam parameters, or calculation errors. When d_{max} is not located at the phantom surface, the impact on the maximum dose remains within approximately 2%, which may account for the limited research on the relationship between bolus material and maximum dose deposition in tissue.

When the ETD does not begin at the phantom surface, the size of the ETD range is not significantly affected by the bolus material, but the starting depth is not completely consistent with the effect on the d_{max}, indicating that d_{max} alone is insufficient to evaluate the bolus material's effect on dose deposition. This discrepancy could result in suboptimal tumor dose coverage, particularly at the upper and lower borders of the treatment field. Conversely, when the ETD begins at the phantom surface, the bolus material significantly affects the extent of the ETD region. For a given bolus thickness, silica gel yields a smaller effective therapeutic region than glycerol, water, or polystyrene. These findings suggest that, as an alternative to radionuclide therapy, selecting an appropriate bolus material and thickness to initiate the ETD at the body surface and terminate it at the corresponding depth of the ^{90}Sr β-particle [24] range could optimize treatment. The characteristics of electron beam dose deposition suggest that the dose rapidly declines, minimizing exposure to deeper tissues, which may reduce the environmental impact associated with radionuclide use. However, challenges to this approach include X-ray contamination from the electron beam [26] and the presence of skin-bolus gaps.

The ideal scenario after the ETD involves a rapid dose decline, as lower doses in this region enhance normal tissue protection. In this study, the four bolus materials showed significant differences in dose deposition in the post-ETD region. Silica gel generally produced higher dose deposition than water, glycerol, and polystyrene. As the electron beam energy decreases and the bolus thickness increases, the dose differences in this region become more significant. This is in agreement with the results obtained from other studies [26].Therefore, careful selection of bolus material is essential to reduce the side effects of radiotherapy and the risk of secondary malignancies in radiation-sensitive tissues beyond the target volume.

These effects directly relate to electron interactions within different materials. This study confirmed that electrons primarily lose energy via ionization and excitation in the four materials, which strongly correlates with electron density. Additionally, a portion of the energy is converted to X-rays through bremsstrahlung, with its intensity positively correlated with the material's effective atomic number [27]. For instance, polystyrene, which has the lowest effective atomic number (5.637) among the tested materials, exhibited the lowest relative dose in the region after the ETD.

With ongoing advancements in materials science, numerous substances are now available for constructing radiotherapy boluses. Due to time limitations, this study did not encompass all materials. While previous studies have primarily focused on air gaps between the bolus and skin [2-10], the increasing accuracy of dose calculations necessitates comprehensive evaluation of bolus material effects on dose distribution. Selecting an appropriate bolus material is essential to ensure adequate tumor dosing while minimizing damage to surrounding tissues. This strategy can reduce patient side effects and secondary cancer risks, ultimately maximizing the therapeutic benefits of modern radiotherapy technologies. Although Monte Carlo methods provide a more accurate reflection of the impact of bolus materials on dose deposition, modern radiotherapy primarily calculates dose deposition in the human body using TPS. However, the effect of bolus materials on the accuracy of different TPS calculations has yet to be explored.

CONCLUSION

The impact of bolus materials on both the ETD and subsequent dose deposition must be carefully considered to ensure sufficient tumor irradiation while minimizing exposure to surrounding tissues.

***Acknowledgment*:** We would like to thank TOPEDIT (https://www.topeditsci.com) for the English language editing.

Conflict of interest: The authors declare that there is no conflict of interest regarding the publication of this paper.

Funding: Scientific Research Project of Wuxi Commission of Health (Z202416).

Ethical considerations: For this article no studies with human participants or animals were performed by any of the authors.

Authors' contribution: D.K.: Investigation, methodology, resources, modeling, computation, writing - original draft; L.H.: Resources, methodology, supervision, data curation and formal analysis; B.Y.: Investigation and data curation; J.H.: Visualization and validation; Y.Z.: Supervision and writing - review & editing; K.G.: Conceptualization, methodology, project administration, and funding acquisition.

[DOI: 10.61186/ijrr.24.1.4]

REFERENCES

1. Monti AF, Brambilla MG, Sarno L, Carbonini C, Ferrari MB, Zanni D, *et al.* (2016) Bolus in optimizing VMAT breast treatments. *Physica Medica,* ***32****: 238.*
2. Wang J-F, Li D-Y, Huang Z-L, *et al.* (2016) Simulation and application of 3D printed compensator in electron radiation therapy for Merkel cell carcinoma. *Chin J Radiat Oncol,* ***9****(25): 999-1002.*
3. Li G, Kuo L, Kowalski A, *et al.* (2019) Clinical evaluation of soft 3D-printed bolus in radiotherapy of nasal cancer. *Int J Radiat Oncol,* **105***(1): E686.*
4. Sharma SC and Johnson MW (1993) Surface dose perturbation due to air gap between patient and bolus for electron beams. *Medical Physics,* ***20****: 20*
5. Huang CY, Yang B, Lam WW, *et al.* (2021) Effects on skin dose from unwanted air gaps under bolus in an MR-guided linear accelerator (MR-LINAC) system. *Physics in Medicine & Biology,* ***66****(6): 065021 (8pp).*
6. Mahdavi JM, Petersen TH, M Sjölin, *et al.* (2015) PO-0838: Determination of the effect on patient surface dose from unwanted air cavities under bolus in VMAT. *Radiother Oncol,* ***115****: S424-S424.*
7. Su S, Moran K, Robar JL (2014) Design and production of 3d printed bolus for electron radiation therapy. *Journal of Applied Clinical Medical Physics,* ***15****(4): 194-211.*
8. Song R and Li W (2023) 3D printed customized bolus for intensity-modulated radiotherapy in a patient with nasal radiotherapy. *International Journal of Radiation Research,* ***21****(1): 153-157.*
9. Won Y and Kim S (2025) Usefulness of cast-type bolus produced by 3D printing for photon beam treatment of primary cutaneous lymphoma: A phantom experiment. *International Journal of Radiation Research,* ***23****(1): 69-75.*
10. Wang KM, Rickards AJ, Bingham T, Tward JD, Price RG (2022) Technical note: evaluation of a silicone-based custom bolus for radiation therapy of a superficial pelvic tumor. *Journal of Applied Clinical Medical Physics,* ***23****(4), e13538.*
11. Lu Y, Shi Q-Y, Wang Y, *et al.* (2022) Research progress on bolus materials used for radiotherapy. *Chin J Radiat Oncol,* ***31****(5): 488-492.*
12. Kim KH, Kang SW, Shin DS, *et al.* (2020) Characteristics of megavoltage electron beams directed through silicone for bolus electron therapy. *J Korean Phys Soc,* ***76****(2): 182-189.*
13. Okoh FU, Yusof MFM, Abdullah R, Kabir NA (2020) Polyvinyl alcohol (pva) based bolus material for high energy photons and electrons. *IOP Conference Series Materials Science and Engineering,* ***785****: 012043.*
14. Araki F (2017) Dosimetric properties of a Solid Water High Equivalency (SW557) phantom for megavoltage photon beams. *Phys Med,* ***39****: 132-136.*
15. Arbor N, Gasteuil J, Noblet C, et al. (2019) A GATE/Geant4 Monte Carlo toolkit for surface dose calculation in VMAT breast cancer radiotherapy. *Phys Med,* ***61****: 112-117.*
16. J. Leste, T. Younes, M. Chauvin, et al. (2018) 36 Monte Carlo simulation of absorbed dose distribution for electron beam using GATE/GEANT4. *Phys Med,* ***56****(Supplement 1): 21.*
17. H.J. Choi, H. Park, W.G. Shin, et al. (2018) EP-1757: Validation of Independent IMRT and VMAT Dose Calculation System based on Geant4 Monte Carlo Toolkit. *Radiotherapy and Oncology,* ***127*** *(Supplement 1): S942.*
18. Geant4 Collaboration (2020) Geant4 Material Database**.** https://geant4-userdoc.web.cern.ch/UsersGuides/ForApplicationDeveloper/BackupVersions/V10.7/html/Appendix/materialNames.html
19. Capote R (2011) Phase-space database for external beam radiotherapy. International Atomic Energy Agency https://www-nds.iaea.org/phsp/electron1/
20. Brualla L, Palanco-Zamora R, Duch MA, Sempau J (2011) Varian_Clinac_2100CD_6MeV_10×10.IAEAheader. International Atomic Energy Agency, https://www-nds.iaea.org/phsp/electron1/Varian_Clinac_2100CD_6MeV_10x10.IAEAheader
22. Khan FM, Doppke KP, Hogstrom KR, Kutcher GJ, Nath R, Prasad SC, *et al.* (1991) Clinical electron-beam dosimetry: report of AAPM radiation therapy committee task group no. 25. *Medical Physics,* ***18****(1): 73-109.*
23. Akima H (1970) A New Method of Interpolation and Smooth Curve Fitting Based on Local Procedures. *Journal of the ACM,* ***17****(4): 589-602.*
24. Takei Y, Takei Y, Monzen H, Tamura M, Kamomae T, Nakaya T, *et al.* (2020) Feasibility of using tungsten functional paper as a thin bolus for electron beam radiotherapy. *Australasian Physical & Engineering Sciences in Medicine,* ***43****(3): 1101-1111.*
25. Chen Y, Chen M-H, Li D, *et al.* (2025) Chinese expert consensus on the treatment of keloids via radionuclide application therapy. *Int J Radiat Med Nucl Med,* ***49****(5): 299-306.*
26. Hensley FW, Major G, Edel C, *et al.* (2014) Technical and dosimetric aspects of the total skin electron beam technique implemented at Heidelberg university hospital. *Reports of Practical Oncology & Radiotherapy,* ***19****(2): 135-143.*
27. Kong D, Wu J, Kong X-D, *et al.* (2024) Effect of bolus materials on dose deposition in deep tissues during electron beam radiotherapy. *Journal of Radiation Research,* ***65****(2): 215-222.*
28. Hu Y-M (1999) Radiation oncology physics. Beijing: Atomic Energy Press.

[DOI: 10.61186/ijrr.24.1.4]